















RESEARCH ARTICLE

Investigating reliable amyloid accumulation in Centiloids:
Results from the AMYPAD Prognostic and Natural History
Study

Ariane Bollack¹  | Lyduine E. Collij^{2,3,4}  | David Vález García²  |
 Mahnaz Shekari^{5,6,7}  | Daniele Altomare⁸  | Pierre Payoux^{9,10} | Bruno Dubois¹¹ |
 Oriol Grau-Rivera⁵ | Mercè Boada^{12,13}  | Marta Marquie^{12,13}  |
 Agneta Nordberg^{14,15} | Zuzana Walker^{16,17}  | Philip Scheltens¹⁸ |
 Michael Schöll^{19,20,21} | Robin Wolz²² | Jonathan M. Schott²³ | Rossella Gismondi²⁴ |
 Andrew Stephens²⁴  | Christopher Buckley²⁵ | Giovanni B. Frisoni⁸ |
 Bernard Hanseeuw^{26,27,28}  | Pieter Jelle Visser^{2,14,29} | Rik Vandenberghe³⁰ |
 Alexander Drzezga^{31,32,33} | Maqsood Yaqub² | Ronald Boellaard^{2,34} |
 Juan Domingo Gispert^{5,6,35}  | Pawel Markiewicz^{1,36}  | David M. Cash^{37,38}  |
 Gill Farrar²⁵ | Frederik Barkhof^{1,2,37}  | On behalf of the AMYPAD consortium

Correspondence

Ariane Bollack, Centre for Medical Image Computing (CMIC), Department of Medical Physics and Bioengineering, University College London, 90 High Holborn, London WC1V 6LJ London, UK.
Email: rmapbol@ucl.ac.uk

Funding information

EPSRC-funded UCL Centre for Doctoral Training in Intelligent, Integrated Imaging in Healthcare (i4health), Grant/Award Number: EP/S021930/1; Department of Health's NIHR-funded Biomedical Research Centre at University College London; NIHR Biomedical Research Centre at UCLH; Alzheimer's Disease Data Initiative (ADDI); GE HealthCare; Innovative Medicines Initiative 2, Grant/Award Number: 115952

Abstract

INTRODUCTION: To support clinical trial designs focused on early interventions, our study determined reliable early amyloid- β ($A\beta$) accumulation based on Centiloids (CL) in pre-dementia populations.

METHODS: A total of 1032 participants from the Amyloid Imaging to Prevent Alzheimer's Disease-Prognostic and Natural History Study (AMYPAD-PNHS) and Insight46 who underwent [¹⁸F]flutemetamol, [¹⁸F]florbetaben or [¹⁸F]florbetapir amyloid-PET were included. A normative strategy was used to define reliable accumulation by estimating the 95th percentile of longitudinal measurements in subpopulations ($N_{\text{PNHS}} = 101/750$, $N_{\text{Insight46}} = 35/382$) expected to remain stable over time. The baseline CL threshold that optimally predicts future accumulation was investigated using precision-recall analyses. Accumulation rates were examined using linear mixed-effect models.

RESULTS: Reliable accumulation in the PNHS was estimated to occur at >3.0 CL/year. Baseline CL of 16 [12,19] best predicted future $A\beta$ -accumulators. Rates of amyloid accumulation were tracer-independent, lower for APOE $\epsilon 4$ non-carriers, and for subjects with higher levels of education.

This is an open access article under the terms of the [Creative Commons Attribution](https://creativecommons.org/licenses/by/4.0/) License, which permits use, distribution and reproduction in any medium, provided the original work is properly cited.

© 2024 The Authors. *Alzheimer's & Dementia* published by Wiley Periodicals LLC on behalf of Alzheimer's Association.

DISCUSSION: Our results support a 12–20 CL window for inclusion into early secondary prevention studies. Reliable accumulation definition warrants further investigations.

KEYWORDS

Alzheimer's, amyloid, Centiloid, longitudinal PET, quantification, reliable accumulation

1 | BACKGROUND

Accumulation of cerebral amyloid beta ($A\beta$) plaques is a key early marker of Alzheimer's disease (AD) pathophysiology, starting decades before the first symptoms appear.¹ Sharp reductions of $A\beta$ were observed in recent lecanemab and donanemab trials in patients with early cognitive impairment who were selected to be amyloid positive.^{2–4} However, it is unknown how these anti- $A\beta$ therapies will affect individuals before symptom onset. This long preclinical phase is the focus of recent secondary prevention trials with anti- $A\beta$ therapy such as the A4 and AHEAD 3-45 studies,^{5,6} which aim to remove incipient aggregates or limit future accumulation.^{7,8} Longitudinal positron emission tomography (PET) studies enable the detection and quantification of small changes in $A\beta$ over time, which is an important outcomes of these trials.⁹ This is supported by recent studies that showed that the rate of $A\beta$ accumulation, rather than baseline burden, improved prediction of cognitive decline in preclinical populations.^{10–12} Identifying early subjects that will accumulate $A\beta$ in the near future can help select those most likely to reach amyloid positivity and benefit from treatment now that successful therapies are becoming available.¹³

While rates of change in $A\beta$ deposition are commonly measured using annualized rates of change in standard uptake value ratio (SUVR), the Centiloid scale (CL) is increasingly being used to minimize differences arising from multiple centers and tracers, including in the latest phase III trials of aducanumab,¹⁴ lecanemab² and donanemab.^{3,4,15} The CL approach was introduced in 2015 as a means of calibrating measures of $A\beta$ deposits to a tracer-independent unbounded scale, where 0 (value characteristic of young healthy controls) and 100 (typical AD subjects) act as anchor points.¹⁶ Longitudinal trajectories of $A\beta$ accumulation have been previously described,^{1,17,18} with more recent studies using the CL scale to characterize the pathophysiological rates of $A\beta$ increase.^{19–25} Although visual reading is currently the approved method for image interpretation in clinical practice (requiring a binary classification of normal/abnormal), the importance of quantifying PET measurement and its uncertainty has been highlighted in the latest Radiological Society of North America Quantitative Imaging Biomarkers Alliance (QIBA) profile.²⁶ Quantitative information generated by CE-marked software can also now be used as an adjunct to visual interpretation.^{27–29} Hence, there is a need for estimates of longitudinal PET changes in CL units that account for measurement uncertainty and intrinsic variability to determine reliable $A\beta$ accumulation trajectories.

Quantification of amyloid burden in “absolute” units can be leveraged into the definition of threshold differentiating stages of amyloid

pathology that are comparable across centers and tracers. So far, using mostly cross-sectional data, various CL thresholds and windows have been established based on histopathology,^{30–32} visual read,^{19,33–37} agreement with other amyloid biomarkers,³⁸ and disease stage.^{30,39} These thresholds have been established to reflect the earliest signs of the presence of $A\beta$ compared to post-mortem studies (~10–12 CL), and compared to visual reads (~16–26 CL) (summary in Pemberton et al.⁹). Finally using longitudinal data from cognitively unimpaired individuals at baseline, the optimal baseline threshold for predicting an abnormal increase in $A\beta$ using PiB was found to be 17.5 CL in the Harvard Aging Brain Study (HABS), 15.0 CL in the Australian Imaging, Biomarker & Lifestyle Flagship Study of Ageing (AIBL),²⁵ and 19 ± 7 CL in the Mayo Clinic Study of Aging (MCSA).²⁴ A [¹⁸F]florbetapir (FBP) threshold of 16.7 CL was also defined using data from the Alzheimer's Disease Neuroimaging Initiative (ADNI).²⁵ However, the definition and robustness of such a threshold for [¹⁸F]flutemetamol (FMM) and [¹⁸F]florbetaben (FBB) remains to be explored.

To further support clinical trial designs that are focused on early intervention, the present study aimed to characterize early $A\beta$ accumulation based on CL units for FMM and FBB in a pre-dementia population, by (1) estimating the variability of longitudinal CL measurements in a population expected to remain stable over time in order to define reliable accumulation beyond measurement error, (2) establishing the baseline CL threshold that optimally predicts future accumulation, and (3) describing the rates of $A\beta$ accumulation across the whole population and investigating their relation to visual read status over time.

2 | METHODS

2.1 | Cohorts

2.1.1 | AMYPAD-PNHS

The present work uses clinical and imaging data from the European Amyloid Imaging to Prevent Alzheimer's Disease (AMYPAD, <https://amypad.eu/>) Prognostic and Natural History Study (PNHS),⁴⁰ downloaded from the Alzheimer's disease data initiative workbench (version v202306, <https://doi.org/10.5281/zenodo.8017084>). The AMYPAD consortium was initiated in 2016 as part of the Innovative Medicine Initiative-Alzheimer's disease platform.⁴¹ The AMYPAD-PNHS is a prospective, multi-center, pan-European study, focused on using amyloid PET to further our understanding of AD in its pre-dementia phase.

RESEARCH IN CONTEXT

- 1. Systematic review:** The authors reviewed the literature using traditional sources, focusing on dementia-related research studies involving longitudinal amyloid positron emission tomography (PET), specifically the ones using the Centiloid (CL) scale. While many studies report the change in amyloid deposition over time, the rate of change that can reliably be considered an increase in amyloid remains unclear.
- 2. Interpretation:** Our findings suggest that a rate of change of 3 CL/year or more can be considered reliable accumulation. They also support a CL window of 12–20 for inclusion into early secondary prevention studies.
- 3. Future directions:** Our results should be further validated in datasets representing the whole AD *continuum*. The notion of reliable accumulation should be investigated according to the tracer, and should consider potential changes in scanner or tracer.

Clinical and imaging data were collected from 11 parent cohorts with similar characteristics (EudraCT 2018-002277-22). Inclusion criteria were as follows: the participant (1) should be non-demented (i.e., Clinical Dementia Rating global score (CDR) ≤ 0.5), (2) older than 50 years of age, (3) able to undergo MRI and PET-acquisition, and (4) active or previously enrolled in a Sponsor-approved parent cohort.

The current analysis included participants who underwent longitudinal PET imaging ($N = 750$ with one PET follow-up, time interval: 3.4 ± 1.9 years; $N = 96$ with two PET follow-ups, time interval at follow-up 2: 5.2 ± 0.7 years).

2.1.2 | Insight46

In order to validate estimates of reliable accumulation in a separate cohort, 282 subjects from Insight46, a prospective neuroscience sub-study of the MRC National Survey of Health and Development,⁴² with baseline and follow-up dynamic PET-MR scans (follow-up time: 2.4 ± 0.2 years) acquired with [¹⁸F]florbetapir were included. All study members were born in the same week of 1946 and the majority were cognitively normal.

2.2 | PET acquisition

2.2.1 | AMYPAD PNHS

PET data were acquired using either FMM ($N = 481$, 64%) or FBB ($N = 269$, 36%). In accordance with the tracers' image acquisition guidance, four frames of 5 minutes were acquired starting at 90 minutes

post-injection of $185 \text{ MBq} \pm 10\%$ of FMM²⁸ or $300 \text{ MBq} \pm 10\%$ of FBB.²⁷ An image harmonization protocol was implemented to ensure that quantitative metrics were comparable across centers,⁴³ resulting in a final effective image resolution of 8 mm across scanners. No partial volume correction was applied.

2.2.2 | Insight46

Images were acquired on the same Biograph mMR 3T PET/MRI scanner (Siemens Healthcare, Erlangen). The full study protocol is described elsewhere.⁴² In short, 370 MBq of FBP was injected intravenously, after which PET data were acquired continuously for ~ 60 min. Only static analysis was used in this study and relied on the last ~ 10 minutes of scanning (from 50 to 60 minutes). Attenuation correction was performed using a pseudo-CT generated from the MR.⁴⁴ Images were smoothed with a 4 mm Gaussian kernel and no partial volume correction was applied.

2.3 | Image processing

2.3.1 | AMYPAD PNHS

First, the quality of the scans was manually assessed. Scans that were deemed to be of sufficient quality were then processed using IXICO's in-house fully automated MR-based PET workflow. Briefly, PET frames were co-registered to create an average image that was aligned to the subject's T1 weighted (T1w) image. Global cortical average and whole cerebellum uptakes were computed from the corresponding GAAIN masks (<http://www.gaain.org/centiloid-project>) from which SUVr values were derived. Following the reference pipeline,¹⁶ SUVr values were converted into appropriate tracer-specific CL metrics.⁴⁵

2.3.2 | Insight46

The Centiloid pipeline used in Insight46 also followed the reference pipeline by Klunk et al.¹⁶ Details of the implementation can be found in Coath et al.⁴⁶

2.4 | Visual reads

PNHS images were classified as either positive (VR+: binding in one or more cortical brain regions unilaterally, as well as striatum for FMM) or negative (VR-: predominantly white matter uptake) by certified nuclear physicians or radiologists according to criteria defined by the manufacturers (Life Molecular Imaging for NeuraCeq and GE HealthCare for Vizamy). Based on VR status over time, subjects were categorized as Stable VR- (VR- at baseline and follow-up), Converters (VR- at baseline and VR+ at the first or the second follow-up), or

Stable VR+ (VR+ at baseline and follow-up). Twelve participants had a VR+ at baseline and VR– during follow-ups.

2.5 | Statistical analyses

R version 4.3.0 (R Program for Statistical Computing) was used for all statistical analyses.

2.5.1 | Definition of reliable accumulation

To assess longitudinal CL uncertainty, a subset of the overall study population was identified to form a reference group, with individuals expected not to accumulate A β over time.

For the PNHS, inclusion criteria for the reference group were as follows: baseline CL negative (<12), baseline and follow-up VR negative, CSF A β 42/40, or A β 42 negative (measures and thresholds were either cohort-specific or based on assay specifications), and CSF p-tau negative, resulting in the selection of 101 individuals. All CSF measures were taken within 1 year of the baseline PET acquisition or during follow-ups.

This approach was replicated in Insight46 by subjects according to the following criteria: at follow-up, CSF A β 42/40 value in the top quartile or normality and normal CSF ptau181 (≤ 57 pg/mL using cut-off from the manufacturer and further validated⁴⁷), no mild cognitive impairment or major brain disorder at baseline (based clinical consensus criteria⁴⁸), yielding 16 individuals.

The definition of reliable accumulation and therefore the classification of individuals as A β -accumulators or non-accumulators was based on an individual annualized rate of change (ARC) being greater than the 95th percentile of the mean ARC in the reference population. Alternatively, we also investigated the use of Gaussian mixture modeling (GMM, $k = 2$ Gaussian distributions) to define reliable accumulation and A β -accumulators as individuals with an ARC greater than the 99th percentile of the first component (corresponding to the mode with the lowest ARC).

2.5.2 | Precision-recall analysis

The baseline CL threshold that best predicts future A β accumulation and VR conversion was established through precision-recall analysis, maximizing the F1-score (i.e., the harmonic mean of the precision and recall). In order to inform secondary prevention trials, a similar analysis excluding individuals with a positive VR at baseline was performed. Bootstrap resampling was used both to optimize the threshold (500 repetitions) and derive its 95% confidence interval (CI; validation using out-of-sample predictions from 1000 repetitions). Three additional scenarios were investigated by setting a minimum precision and recall of 0.7 and a minimum specificity of 0.9. A precision-recall analysis was preferred to a receiver operating characteristic analysis as it is better suited for data with imbalanced classes.⁴⁹

2.5.3 | Characterizing longitudinal trajectories

Longitudinal trajectories of A β accumulation were modeled by fitting a linear mixed effect model (LME) to the whole cohort (*lmer* 1.1.33 package in R) with CL as the outcome measure. The first model included the effect of time, group (i.e., PNHS reference/study group) and the interaction between the two, allowing for group-specific random effects (with an unstructured covariance matrix). For the study group, fitting included random intercepts and slopes, while for the reference group we allowed random intercepts only in order not to overfit the model.

The effect of known risk factors and tracer on both baseline and changes in CL over time were then investigated in the following order: baseline age, APOE- ϵ 4 carriership, PET tracer, sex, and education (as categorical variable: compulsory/upper-secondary/post-secondary education). These factors and their interaction with time were kept in subsequent models if they improved the fit of the model, assessed using the corrected Akaike information criterion, and if their effect on CL burden was statistically significant.

We then investigated whether CL load at baseline and the annualized CL accumulation differed across VR status over time (i.e., Stable VR–/Converters/Stable VR+) and cognitive state (i.e., Cog: cognitively unimpaired (CDR = 0)/cognitive impaired (CDR \geq 0.5)). For this analysis, only Converters from VR– to VR+ were included.

Bootstrap resampling from 1000 samples was used to derive 95% confidence intervals of model estimates.

2.6 | Data and code availability

Data used in the preparation of this article were obtained from the AMYPAD PNHS dataset, (version v202306, <https://doi.org/10.5281/zenodo.8017084>). The R code use for the analysis can be found on Zenodo (<https://doi.org/10.5281/zenodo.10808658>).

3 | RESULTS

3.1 | Demographics

Demographic characteristics for the whole cohort are summarized in Table 1. The PNHS dataset comprised 750 pre-dementia subjects with longitudinal amyloid-PET imaging. Participants had a median age of 65 years (range = 49 to 96 years), 57% were females, 41% were APOE- ϵ 4 carriers, and 18% had baseline VR+ scan. Individuals with FMM acquisitions had a lower baseline age compared to those with FBB acquisitions (65.3 ± 8.0 vs. 66.4 ± 6.9 years, $p < 0.001$), as well as a higher proportion of APOE- ϵ 4 carriers (FMM = 46%, FBB = 33%, $\chi^2 = 24.52$, $p < 0.001$).

The whole cohort was then split into a reference subset with individuals unlikely to accumulate amyloid over the duration of the study

TABLE 1 Demographic characteristics of the PNHS data, split by tracer.

Variable	Overall, N = 750 ^a	Florbetaben, N = 269 ^a	Flutemetamol, N = 481 ^a	p-value
Age, years	65.7 (7.6)	66.4 (6.9)	65.3 (8.0)	<0.001 ^b
Gender				0.2 ^c
Male	324/750 (43%)	107/269 (40%)	217/481 (45%)	
Female	426/750 (57%)	162/269 (60%)	264/481 (55%)	
APOE ε4 alleles (% carriers)				0.002 ^c
0	429/735 (58%)	173/259 (67%)	256/476 (54%)	
1	270/735 (37%)	73/259 (28%)	197/476 (41%)	
2	36/735 (5%)	13/259 (5%)	23/476 (5%)	
(Missing)	15	10	5	
VR category				0.12 ^d
Stable VR–	562/750 (75%)	211/269 (78%)	351/481 (73%)	
Converters+ (VR– > VR+)	56/750 (7%)	17/269 (6%)	39/481 (8%)	
Converters– (VR+ > VR–)	12/750 (2%)	1/269 (0%)	11/481 (2%)	
Stable VR+	120/750 (16%)	40/269 (15%)	80/481 (17%)	
Education, years				0.003 ^c
Compulsory	133/750 (18%)	54/269 (20%)	79/481 (16%)	
Upper-secondary	218/750 (29%)	58/269 (22%)	160/481 (33%)	
Post-secondary	399/750 (53%)	157/269 (58%)	242/481 (50%)	
CDR				0.007 ^c
0 – Normal	701/747 (94%)	242/267 (91%)	459/480 (96%)	
0.5 – Very mild	46/747 (6%)	25/267 (9%)	21/480 (4%)	
(Missing)	3	2	1	
MMSE	29.2 (1.0)	29.2 (1.0)	29.2 (1.0)	0.6 ^b
(Missing)	59	20	39	
N timepoints				<0.001 ^c
2	654/750 (87%)	173/269 (64%)	481/481 (100%)	
3	96/750 (13%)	96/269 (36%)	0/481 (0%)	
Time interval follow-up 1, years	3.00 (2.10, 4.00)	2.20 (2.00, 2.90)	3.40 (2.60, 4.20)	
Time interval follow-up 2, years	5.30 (5.20, 5.40)	5.30 (5.20, 5.40)	–	
Baseline CL	14.1 (24.6)	12.6 (25.3)	15.1 (24.1)	0.002 ^b
ARC, CL/years	1.5 (3.3)	1.8 (3.7)	1.4 (3.0)	0.4 ^b

Abbreviations: APOE, apolipoprotein E; ARC, annualized rate of change, computed as $(CL_{\max(\text{follow-up})} - CL_{\text{baseline}})/dt$; CL, Centiloid; CDR, Clinical Dementia Rating Global Score, MMSE, Mini-Mental State Examination; VR, visual read.

^aMean (SD); n/N (%).

^bWilcoxon rank sum test.

^cPearson's chi-squared test.

^dFisher's exact test.

(N = 101; including $N_{\text{FMM}} = 86$ and $N_{\text{FBB}} = 15$; mean follow-up time 3.2 years, SD = 0.9, range = 1.4 to 5.2 years) and an exploratory set (N = 649; including $N_{\text{FMM}} = 395$ and $N_{\text{FBB}} = 254$).

In the reference group, the mean baseline amyloid load was 2.4 ± 5.7 CL, compared to 14.1 ± 23.3 CL in the exploratory group, with no significant difference between tracers ($p = 0.2$). No difference in age, sex, APOE-ε4 carriership, or years of education was observed across tracers in this reference group.

3.2 | Defining reliable Aβ accumulation

Reliable Aβ accumulation in the PNHS was defined as an ARC greater than 3.0 CL/year, corresponding to the upper bound of the 95% CI of the ARC in the reference group (Figure 1A). Within the exploratory cohort, individuals were then categorized as Aβ-accumulators and non-accumulators based on whether they surpassed the threshold of reliable accumulation. According to this definition, 27.9% of individuals

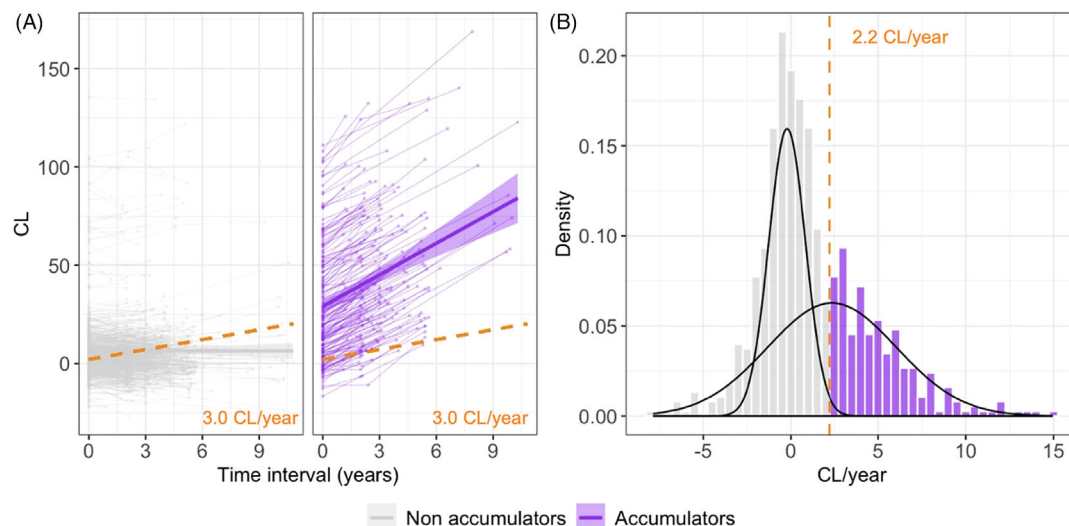


FIGURE 1 Definition of reliable accumulation using two approaches. (A) Reliable accumulation based on the 95th percentile of the annualized CL rate of change in a reference group (i.e., >3.0 CL/year), represented by the orange dotted lines. The plot displays longitudinal CL trajectories within the PNHS exploratory subset, for A β -accumulators (individuals that showed reliable accumulation, in purple) and non-accumulators (in gray). (B) Reliable accumulation based on gaussian mixture modeling ($k = 2$) using the whole PNHS cohort. The orange vertical line represents the 99th percentile of the first Gaussian distribution and corresponds to 2.2 CL/year. ARC, annualized rates of change; CL, Centiloid; PNHS, Prognostic and Natural History Study.

Total	468	181	649
Stable VR+	39	81	120
Converters- (VR+ > VR-)	9	3	12
Converters+ (VR- > VR+)	15	41	56
Stable VR-	405	56	461
	Non accumulators	Accumulators	Total

FIGURE 2 Number of subjects in each category within the exploratory cohort. A β -Accumulators based on the 95th percentile of the annualized CL rate of change in a reference group (i.e., >3.0 CL/year). A β , amyloid- β ; CL, Centiloid; VR, visual reads.

in the exploratory cohort were A β -accumulators. As expected, this number was significantly higher in the Converters and Stable VR+ groups ($44/68 = 64.7\%$ and $81/120 = 67.5\%$, respectively, see count per category in Figure 2). In the Stable VR- group, still 12.1% ($56/461$) were classified as A β -accumulators despite having a shorter follow-up time compared to non-accumulators ($p = 0.006$). A β -accumulators were on average 3 years older than non-accumulators (67.8 ± 7.8 vs. 64.8 ± 7.7 years, $p = 0.001$) and tended to have a higher baseline CL load (8.3 ± 14.1 CL vs. 3.0 ± 8.7 CL, $p = 0.016$). No difference in sex or APOE- $\epsilon 4$ carriership was observed.

Using GMM as an alternative method to define reliable accumulation, the reliable A β accumulation threshold corresponded to an ARC greater than 2.2 CL/year (Figure 1B).

In Insight46, the reliable accumulation estimate was 3.7 CL/year using the 95th percentile of the ARC in the reference group and 3.2 CL/year using the GMM approach. The A β -accumulators had a higher percentage of APOE- $\epsilon 4$ carriers (A β -accumulators = 50%, non-accumulators = 21%, $\chi^2 = 39.01$, $p < 0.001$) and females (A β -accumulators = 45%, non-accumulators = 56%, $\chi^2 = 4.64$, $p = 0.04$).

3.3 | Optimal threshold to predict future A β -accumulators

To determine the optimal threshold to predict future A β accumulation, a Precision-Recall analysis was used to classify individuals as A β -accumulators or non-accumulators (ARC > 3.0 CL/year) based on their baseline CL load. The resulting threshold and 95% CI were 15.7 [12.4, 19.4] (Figure 3). Importantly, in individuals with a baseline VR-, the threshold is lower (12.9 [8.8, 16.6] CL). FMM threshold was 17.4 [13.7, 21.4], higher than FBB 13.0 [8.5, 18.6], albeit overlapping CI. Using the GMM-based definition of A β -accumulators yields a similar but slightly lower threshold of 12.8 [9.1, 16.5] CL.

Three additional scenarios were investigated by setting a minimum precision, recall and specificity of 0.7 (Figure 4A). While adding a constraint on precision and specificity produces comparable results, increasing recall at the expense of other metrics greatly lowered the threshold to 4.2 [-1.2, 8.7] CL.

Furthermore, the predictive value of baseline CL is higher in APOE- $\epsilon 4$ carriers individuals (precision = 0.72; recall = 0.70, threshold: 12.4

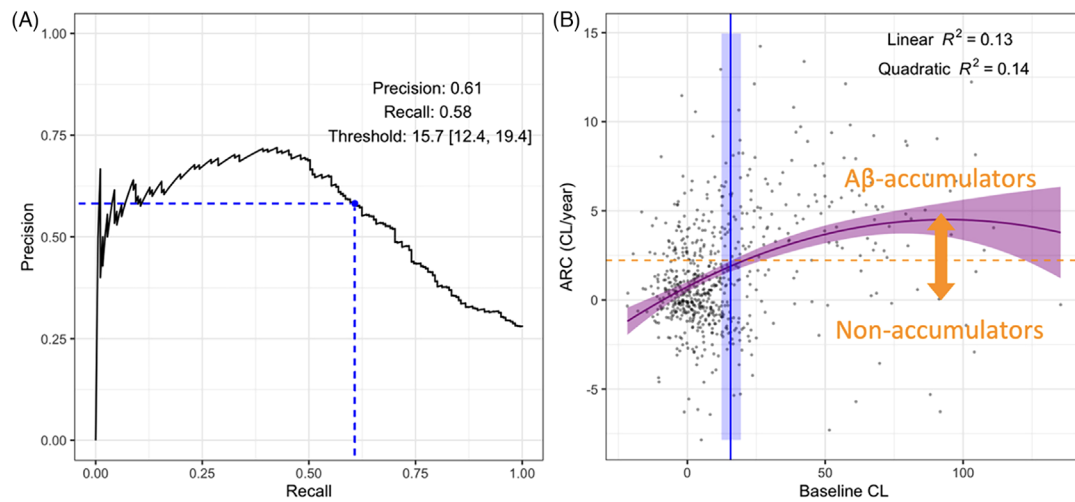


FIGURE 3 (A) Precision-Recall curve using baseline CL load as predictor to identify A β -Accumulators. In blue, the maximum F1 score corresponds to a baseline amyloid load of 15.7 [12.4, 19.4] CL; Bootstrap resampling was used both to optimize the threshold (500 repetitions) and derive its 95% confidence interval (CI; validation using out-of-sample predictions from 1000 repetitions). (B) ARC versus baseline CL load. The blue line represents a baseline threshold of 15.7 CL. The shaded blue area defines the boundaries of the 95% CI around the threshold. The orange line represents the limit above which subjects are considered A β -Accumulators (ARC > 3.0 CL/year). The purple curve represents the data fitted with a quadratic polynomial. A β , amyloid- β ; ARC, annualized rate of change; CI, confidence interval; CL, Centiloid; VR, visual read.

[6.4, 15.9]) (Figure 4B) and for participants scans with FMM (precision = 0.63; recall = 0.63, threshold: 14.3 [10.5, 17.8]) compared to FBB (precision = 0.53) (Figure 4C). Finally, the sensitivity decreased and the specificity increased with higher levels of education (Figure 4D), which also resulted in higher baseline CL thresholds to predict future accumulation (threshold_{compulsory}: 14.0 [6.1, 21.1]; threshold_{upper-secondary}: 15.5 [12.4, 19.6] threshold_{post-secondary}: 18.8 [12.8, 23.7]).

3.4 | Longitudinal A β -PET trajectories

Longitudinal trajectories of amyloid accumulation were characterized using LME. The first model highlighted the differences between exploratory and reference groups, with a higher baseline CL in the former (baseline CL_{exploratory} = 14.0 [12.1, 15.8], baseline CL_{reference} = 2.3 [1.0, 3.5], $t = -10.1$, $p < 0.001$), and by definition a higher average ARC (ARC_{exploratory} = 1.5 [1.3, 1.8] CL/year, ARC_{reference} = -0.2 [-0.5, 0.2], $t = -8.4$, $p < 0.001$).

In a second step, we tested the predictive value of baseline age, APOE- $\epsilon 4$ carriership, PET tracer, sex, education (in this order), and their interaction with time as covariates.

First, baseline age and APOE- $\epsilon 4$ carriership had a significant impact on baseline CL (baseline age: $p < 0.001$; APOE- $\epsilon 4$ carriership: $t = 4.15$, $p < 0.001$); however, only the interaction of APOE- $\epsilon 4$ carriership with time was also predictive of CL accumulation over time (APOE- $\epsilon 4$ carriership*time: $t = 4.21$, $p < 0.001$; baseline age*time: $t = 1.70$, $p = 0.09$). Regarding the tracer, FMM baseline CL estimates were on average approximately five CL higher than the ones for FBB ($t = 3.98$, $p < 0.001$). The interaction between tracer and time was not significant ($t = -1.67$, $p = 0.09$) (Figure 5).

We also found no evidence of sex differences on CL load and CL over time. At this stage, the model included the following risks factors as predictors: baseline age, and APOE- $\epsilon 4$ carriership and its interaction with time. Adding the level of education, however, was predictive of baseline CL load, with an amyloid burden on average 3.6 CL lower for post-secondary education compared to compulsory level of education (post-secondary vs. compulsory $t = -2.31$, $p = 0.02$). Our results also suggest that higher levels of education (upper- or post-secondary) were indicative of slower ARC, on average -0.55 CL/year, compared to compulsory level of education (upper-secondary vs. compulsory $t = -2.02$, $p = 0.04$; post-secondary vs. compulsory $t = -2.15$, $p = 0.032$).

Based on these results, we included baseline age, PET tracer, APOE- $\epsilon 4$ carriership and its interaction with time and the level of education as covariates for subsequent analyses (the interaction between education and time was removed from the model).

Finally, longitudinal CL trajectories across cognitive groups (i.e., cognitively unimpaired/cognitively impaired) and VR over time (i.e., Stable VR-/Converters/Stable VR+) were explored. The cognitive status of individuals based on the CDR was not predictive of CL burden. Baseline CL values and ARC were higher in Stable VR+ and Converters compared to Stable VR- (focusing on differences between Stable VR- and Converters, baseline CL: $t = 5.34$, $p < 0.001$; ARC: $t = 14.62$, $p < 0.001$), but no significant difference in ARC was found between Converters and Stable VR+ ($t = -1.58$, $p = 0.12$) (Figure 5).

4 | DISCUSSION

The present study characterized A β accumulation, as expressed in CL units based on FMM and FBB amyloid-PET in the AMYPAD PNHS pre-

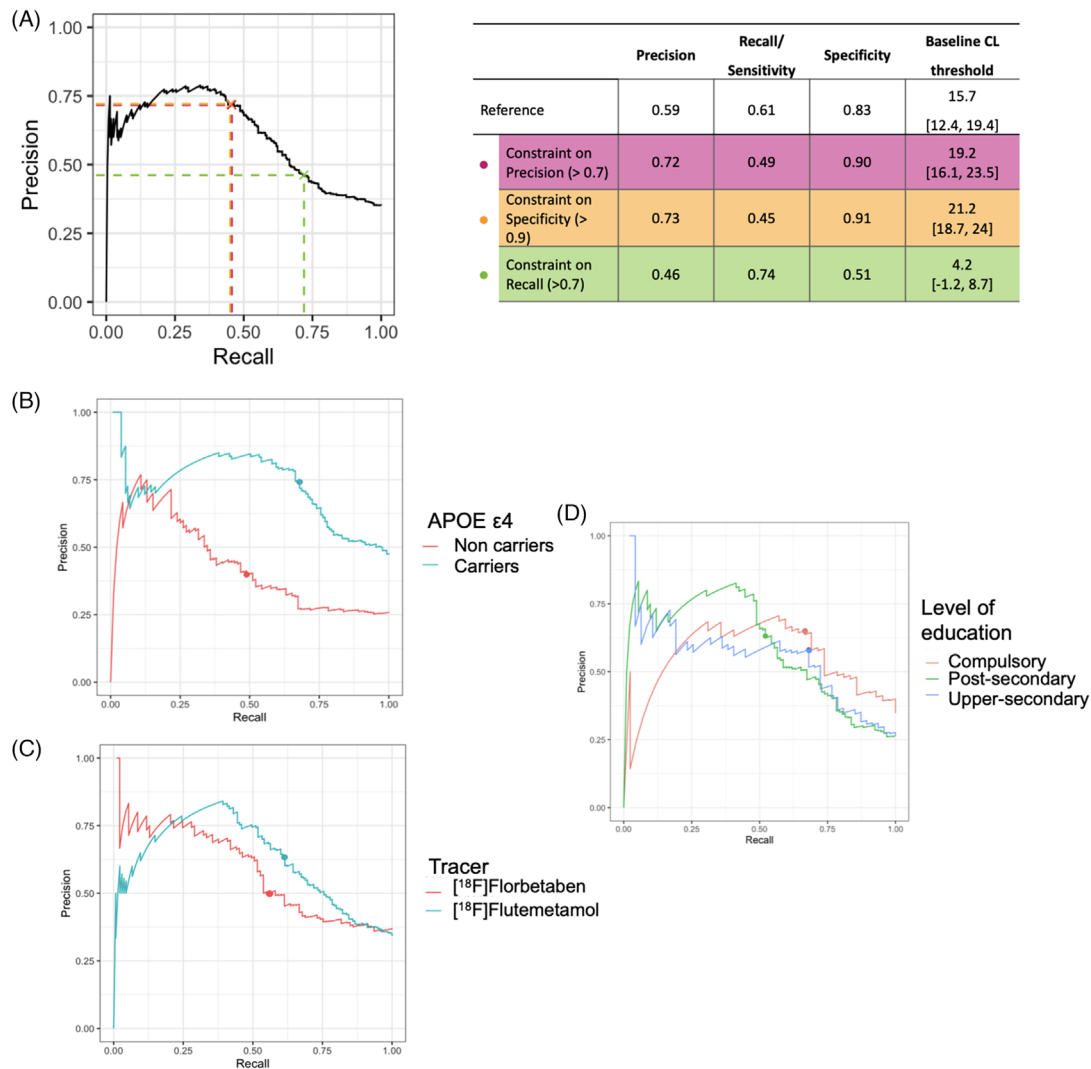


FIGURE 4 Summary of Precision-Recall Analysis using baseline CL to predict reliable accumulation. The optimal baseline CL threshold is determined by maximizing the F1-score. (A) Three additional scenarios were investigated by adding a constraint on precision, recall or specificity (minimum value = 0.7 for precision and recall, 0.9 for specificity). Bootstrap resampling was used both to optimize the threshold (500 repetitions) and derive its 95% confidence interval (CI; validation using out-of-sample predictions from 1000 repetitions). (B, C, D) Precision-Recall curves according to APOE $\epsilon 4$ carriership, tracer, and level of education respectively. APOE, apolipoprotein E; AUC, area under the curve; CL, Centiloid.

dementia population. We first estimated the variability of longitudinal CL measurements in a reference sub-population expected to remain stable over time and defined reliable accumulation as an ARC greater than 3.0 CL/year. In a separate dataset from the Insight46 study, this was estimated at 3.7 CL/year. This notion should be further evaluated using several independent cohorts. We then established that a baseline CL threshold of 16 [12,19] could help identify future $A\beta$ -accumulators (Figure 6). Furthermore, in the PNHS, APOE- $\epsilon 4$ carriers, and those with a lower educational background exhibited faster rates of $A\beta$ accumulation. Notably, among participants with an initial negative VR, those who later had a VR positive scan displayed a higher amyloid burden at baseline (~11 CL) and an increased ARC (~4.4 CL/year) in contrast to participants who consistently tested VR negative throughout their follow-up period.

Several strategies have been previously developed to distinguish $A\beta$ -accumulators from non-accumulators, based on the SUVr and using the inflexion in between peaks of bimodal distribution of the ARC,⁵⁰ or based on the amyloid load and using of k-means clustering and the mean change + 2SD in an $A\beta$ negative group.⁵¹ Whereas these strategies tend to maximize the difference between $A\beta$ -accumulators and non-accumulators, our normative approach to define $A\beta$ -accumulators might be helpful in identifying earlier individuals at greater risk of becoming amyloid positive.

Our study's approach to use a stable reference group for estimating longitudinal variability aligns with the recent QIBA profile²⁶ and has been used in several studies.^{19,51-53} However, our reference group selection criteria were stricter and included CSF amyloid and tau measurements. This could explain why in AIBL for instance, the

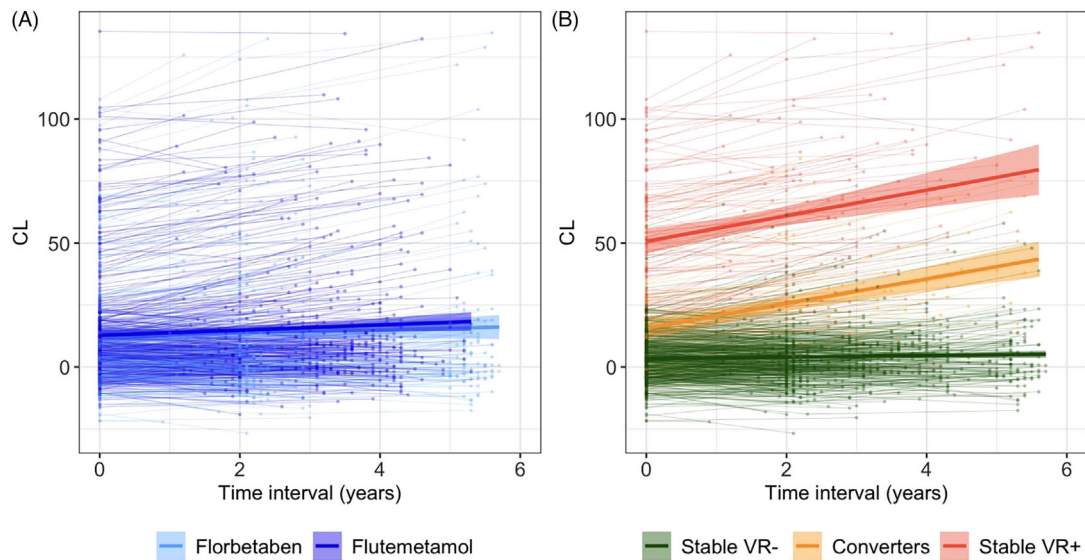


FIGURE 5 Longitudinal trajectories of amyloid accumulation (A) by tracer and (B) based on VR over time. CL, Centiloid scale; VR, visual reads.

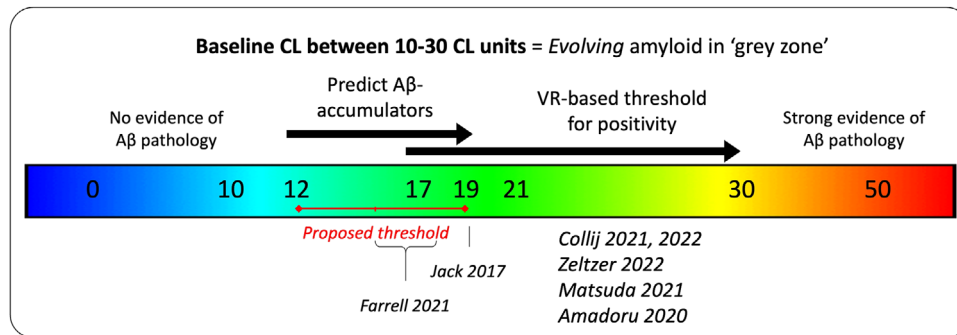


FIGURE 6 Overview of CL thresholds with a focus in the “gray zone,” between 10 and 30 CL. CL, Centiloid; VR, visual reads.

95th percentile absolute change in an amyloid negative group (defined as CL < 20) was 6.56 CL/year (Bourgeat et al.¹⁹) whereas the 95th percentile estimate in our study was 3.0 CL/year. Further investigations are crucial to evaluate the notion of reliable accumulation on which is base the classification of individuals as A β -accumulators or non-accumulators, considering factors such as the tracer used, the reference region, changes in scanner in between timepoints, and registration methods. Additionally, taking into account the population's diversity and the type of dataset is crucial. Indeed, reliable accumulation in curated research datasets might be lower than more heterogeneous clinical datasets. This underscores the need for robustness testing and cautious interpretation in estimating reliable accumulation in future studies.

As longitudinal PET studies using CL become increasingly widespread, establishing a standardized strategy to determine reliable accumulation and A β -accumulators can help better track subthreshold amyloid accumulation and can potentially help assess potential re-accumulation of amyloid after successful treatment.

Numerous CL thresholds have been established to correlate the scale with varying levels of amyloid pathology. Based on post-mortem

studies³⁰ and CSF studies, a CL below 10 units would reliably exclude the presence of amyloid, and a CL load above 30 units would be strong evidence of the presence of amyloid.³⁸ The window between 10 and 30 CL units can be regarded as a “gray zone,” indicative of an evolving pathology trending toward positivity. Indeed, in previous studies, VR-based thresholds typically fell within this gray zone, ranging from 17 CL for expert readers^{33,37} to 26 CL in several studies.^{30,33,54} Our findings suggest that the lower end of the gray zone (~12–20 CL) could represent the optimal window to predict short-term A β accumulation as reflected by a reliable CL increase. These results are in accordance with the work of Farrell et al. who reported an optimal threshold to predict future accumulation varying from 15 to 17.5 CL across AIBL, HABS and ADNI cohorts,²⁵ as well as the reliable worsening estimate of 19 CL determined by Jack et al.²⁴ (Figure 5). In the future, in a clinical setting focused on secondary prevention, a follow-up scan could be considered after 2 years for individuals with a CL above 15 but below 30 units.

Furthermore, we established three scenarios to help inform subject selection strategies. In our precision-recall analysis, by setting a minimum precision and recall of 0.7 and minimum specificity of 0.9, the aim

was to help minimize false positives, help minimize false negatives, or increase our ability to correctly predict non-accumulators. Increasing precision and specificity results in baseline CL thresholds higher than our reference estimate (albeit overlapping confidence intervals) and, therefore, closer to VR-based positivity thresholds. As can be expected, increasing recall markedly decreased baseline CL threshold. Indeed, as the CL burden reflects the cumulative effect of amyloid accumulation over time, a few subjects with a low baseline amyloid burden are also A β -accumulators.

Finally, in assessing the longitudinal CL trajectories over time, two primary factors emerged as influential on the ARC: APOE- ϵ 4 carrier-ship and level of education. Although we found a significant impact of APOE- ϵ 4 carrier-ship on the ARC, this might not be generalizable to cohorts with higher amyloid burden or mostly cognitively impaired individuals.^{23,55,56} Indeed, compared to non-carriers, APOE- ϵ 4 carriers are more likely to accumulate A β pathology and tend to develop the disease earlier.^{57,58} In addition, the level of education is sometimes used as a proxy for conceptualizing resistance to amyloid deposition^{59,60}; however, further studies with more specific markers are warranted to elucidate the potential protective factors against amyloid accumulation. Importantly, our results showed no differences in longitudinal trajectories across tracers, confirming that the CL scale is well-suited for multi-tracer, longitudinal PET studies. Finally, no difference was observed between cognitive groups, which probably reflects that the PNHS (like Insight46) is a preclinical cohort with only 5% of individuals having (very mild) cognitive impairment.

The current study also presents some limitations. First, VR were performed by local readers, so some disagreement is to be expected. Second, the CL is derived from the SUVr, which is a semi-quantitative measure that could be affected by some treatment strategies (e.g., blood flow fluctuations, reference kinetics, tracer clearance). Modifications in these factors will lead to changes in SUVr, independent of any shifts in amyloid levels. Therefore, future trials should reassess the validity of SUVr for each new drug using dynamic PET to perform a full kinetic analysis. Third, the definition of reliable accumulation is linked to the methodology employed to calculate the ARC. If the ARC was determined based on LME estimates, we would expect lower values. Last, our reference subset demonstrated a bias toward FMM, incorporating only 15 FBB scans. Similarly, the Insight46 reference subset consisted of 35 individuals only. To refine our understanding of reliable accumulation, future evaluations should be conducted per tracer and encompass datasets with larger sample sizes.

The present study characterized A β accumulation expressed in CL units using three United States Food and Drug Administration and European Medicines Agency approved fluorinated amyloid tracers in a mainly pre-clinical population. We first presented a normative strategy to define reliable amyloid accumulation by estimating the variability of longitudinal CL measurements (3 CL/year in the PNHS) in a sub-population expected to remain stable over time. We then established a baseline CL of 16 [12,19] to help predict future A β -accumulators. Our results support a CL window of 12–20 for inclusion of subjects into early secondary prevention studies.

AFFILIATIONS

¹Centre for Medical Image Computing (CMIC), Department of Medical Physics and Bioengineering, University College London, London, London, UK

²Department of Radiology and Nuclear Medicine, Amsterdam UMC, Amsterdam, The Netherlands

³Clinical Memory Research Unit, Department of Clinical Sciences, Lund University, Malmö, Sweden

⁴Amsterdam Neuroscience, Brain Imaging, VU University Amsterdam, Amsterdam, The Netherlands

⁵Barcelona β eta Brain Research Center (BBRC), Pasqual Maragall Foundation, Barcelona, Spain

⁶Universitat Pompeu Fabra, Barcelona, Spain

⁷Instituto de investigaciones médicas Hospital del Mar (IMIM), Barcelona, Spain

⁸Neurology Unit, Department of Clinical and Experimental Sciences, University of Brescia, Brescia, Italy

⁹Department of Nuclear Medicine, Imaging Pole, Toulouse University Hospital, Toulouse, France

¹⁰Toulouse Neuroimaging Center, Université de Toulouse, Inserm, UPS, CHU Purpan, Pavillon Baudot, Place du Docteur Joseph Baylac, Toulouse, France

¹¹Department of Neurology, Salpêtrière Hospital, AP-HP, Sorbonne University, Paris, France

¹²Ace Alzheimer Center Barcelona – Universitat Internacional de Catalunya, Barcelona, Spain

¹³CIBERNED, Network Center for Biomedical Research in Neurodegenerative Diseases, National Institute of Health Carlos III, Madrid, Spain

¹⁴Department of Neurobiology, Care Sciences and Society, Center for Alzheimer Research, Division of Clinical Geriatrics, Karolinska Institutet, Stockholm, Sweden

¹⁵Theme Inflammation and Aging, Karolinska University Hospital, Karolinska Institutet, Stockholm, Sweden

¹⁶Division of Psychiatry, University College London, London, UK

¹⁷Essex Partnership University NHS Foundation Trust, The Lodge, Wickford, UK

¹⁸Alzheimer Center and Department of Neurology, Amsterdam Neuroscience, VU University Medical Center, Alzheimercentrum Amsterdam, Amsterdam, The Netherlands

¹⁹Wallenberg Centre for Molecular and Translational Medicine, The University of Gothenburg, Gothenburg, Sweden

²⁰Department of Psychiatry and Neurochemistry, Institute of Neuroscience and Physiology, The Sahlgrenska Academy, University of Gothenburg, Sahlgrenska University Hospital, Gothenburg, Sweden

²¹Department of Neurodegenerative Disease, UCL Institute of Neurology, London, UK

²²IXICO Plc, London, UK

²³Dementia Research Centre, UCL Queen Square Institute of Neurology, London, UK

²⁴Life Molecular Imaging, GmbH, Berlin, Germany

²⁵GE HealthCare, Buckinghamshire, UK

²⁶Department of Neurology, Institute of Neuroscience, Université Catholique de Louvain, Cliniques Universitaires Saint-Luc, Brussels, Belgium

²⁷Gordon Center for Medical Imaging, Department of Radiology, Massachusetts General Hospital, Boston, Massachusetts, USA

²⁸WELBIO Department, WEL Research Institute, Wavre, Belgium

²⁹Alzheimer Center Limburg, School for Mental Health and Neuroscience, Maastricht University, Maastricht, The Netherlands

³⁰Laboratory for Cognitive Neurology, LBI – KU Leuven Brain Institute, Leuven, Belgium

³¹Department of Nuclear Medicine, University Hospital Cologne, Universitätsklinikums Köln, Köln, Germany

³²Molecular Organization of the Brain, Institute for Neuroscience and Medicine, INM-2, Forschungszentrum Jülich GmbH, Jülich, Germany

³³German Center for Neurodegenerative Diseases (DZNE), Bonn, Germany

³⁴Nuclear Medicine and Molecular Imaging, University Medical Center Groningen, University of Groningen, Groningen, The Netherlands

³⁵Centro de Investigación Biomédica en Red de Bioingeniería, Biomateriales y Nanomedicina, Instituto de Salud Carlos III, Madrid, Spain

³⁶Computer Science and Informatics, School of Engineering, London South Bank University, London, UK

³⁷Queen Square Institute of Neurology, University College London, London, UK

³⁸UK Dementia Research Institute at University College London, London, UK

ACKNOWLEDGMENTS

The authors thank Mark Schmidt for his contributions to the AMYPAD consortium. This work is supported by the EPSRC-funded UCL Centre for Doctoral Training in Intelligent, Integrated Imaging in Healthcare (i4health) (EP/S021930/1), the Department of Health's NIHR-funded Biomedical Research Centre at University College London, and GE HealthCare. Frederik Barkhof is supported by the NIHR Biomedical Research Centre at UCLH.

AMYPAD FUNDING: The project leading to this paper has received funding from the Innovative Medicines Initiative 2 Joint Undertaking under grant agreement No 115952. This Joint Undertaking receives the support from the European Union's Horizon 2020 research and innovation programme and EFPIA. This communication reflects the views of the authors and neither IMI nor the European Union and EFPIA are liable for any use that may be made of the information contained herein. The AMYPAD PNHS is registered at www.clinicaltrialsregister.eu with the EudraCT Number: 2018-002277-22. This work was supported by the Alzheimer's Disease Data Initiative (ADDI).

CONFLICT OF INTEREST STATEMENT

A.B., C.B., and G.F. are employees of GE HealthCare. L.C. has received research support from GE HealthCare (paid to institution). D.A. received funding by the Swiss National Science Foundation (project CRSK-3_196354/1). OG-R receives research support from F. Hoffmann-La Roche Ltd. and has given lectures in symposia sponsored by Roche Diagnostics. M.B. received research funding from the Instituto de Salud Carlos III (ISCIII) Acción Estratégica en Salud, integrated in the Spanish National RCDCI Plan and financed by ISCIII-Subdirección General de Evaluación and the Fondo Europeo de Desarrollo Regional (FEDER—Una manera de hacer Europa) grant PI17/01474, and the European Union/EFPIA Innovative Medicines Initiative Joint MOPEAD project (grant number 115985). M.M. reports research funding from the Instituto de Salud Carlos III (ISCIII) Acción Estratégica en Salud, integrated in the Spanish National RCDCI Plan and financed by ISCIII-Subdirección General de Evaluación and the Fondo Europeo de Desarrollo Regional (FEDER—Una manera de hacer Europa) grant PI19/00335, travel support from F. Hoffmann-La Roche

Ltd. and participation on the Spanish Scientific Advisory Board for biomarkers from Araclon-biotech—Grifols. M.Sch. has served on scientific advisory boards for Servier Pharmaceuticals, NovoNordisk and Roche, and has received funding from Roche, Novo Nordisk and Bioarctic (paid to institution), all outside the scope of this study. RW is an employee of IXICO. J.M.S. has received research funding and PET tracer from AVID Radiopharmaceuticals (a wholly owned subsidiary of Eli Lilly) and Alliance Medical; has consulted for Roche, Eli Lilly, Biogen, AVID, Merck, and GE; and received royalties from Oxford University Press and Henry Stewart Talks. He is Chief Medical Officer for Alzheimer's Research UK, and Medical Advisor to UK Dementia Research Institute. R.G. is a full-time employee of Life Molecular Imaging GmbH, Berlin, Germany. A.D. reports the following: Research support from Siemens Healthineers, Life Molecular Imaging, GE Healthcare, AVID Radiopharmaceuticals, Sofie, Eisai, Novartis/AAA, Ariceum Therapeutics; Speaker Honorary/Advisory Boards: Siemens Healthineers, Sanofi, GE Healthcare, Biogen, Novo Nordisk, Invicro, Novartis/AAA, Bayer Vital; Stock: Siemens Healthineers, Lantheus Holding, Structured therapeutics, ImmunoGen; Patents: Patent for 18F-JK-PSMA-7 (PSMA PET imaging tracer, Patent No.: EP3765097A1; Date of patent: Jan. 20, 2021). J.D.G. reports research support from GE Healthcare, Roche Diagnostics, and Hoffmann-La Roche; has given lectures in symposia sponsored by General Electrics, Philips Netherlands, Life Molecular Imaging, and Biogen; has served on scientific advisory boards or as a consultant for Prothena Biosciences and Roche Diagnostics; and is the inventor, founder, and co-owner of BetaScreen. F.B. is a steering committee or iDMC member for Biogen, Merck, Roche, EISAI and Prothena. He is a consultant for Roche, Biogen, Merck, IXICO, Jansen, Combinostics and has research agreements with Merck, Biogen, GE Healthcare, Roche. He is co-founder and shareholder of Queen Square Analytics LTD. The remaining authors have no conflicts of interest to declare. Author disclosures are available in the [Supporting information](#).

CONSENT STATEMENT

All human subjects provided informed consent.

ORCID

Ariane Bollack  <https://orcid.org/0000-0002-9169-7530>

Lyduine E. Collij  <https://orcid.org/0000-0001-6263-1762>

David Vázquez García  <https://orcid.org/0000-0003-3308-3167>

Mahnaz Shekari  <https://orcid.org/0000-0003-1336-6768>

Daniele Altomare  <https://orcid.org/0000-0003-1905-8993>

Mercè Boada  <https://orcid.org/0000-0003-2617-3009>

Marta Marquíe  <https://orcid.org/0000-0002-0660-0950>

Zuzana Walker  <https://orcid.org/0000-0001-7346-8200>

Andrew Stephens  <https://orcid.org/0000-0001-5052-6586>

Bernard Hanseeuw  <https://orcid.org/0000-0002-3102-6778>

Juan Domingo Gispert  <https://orcid.org/0000-0002-6155-0642>

Pawel Markiewicz  <https://orcid.org/0000-0002-3114-0773>

David M. Cash  <https://orcid.org/0000-0001-7833-616X>

Frederik Barkhof  <https://orcid.org/0000-0003-3543-3706>

REFERENCES

- Villemagne VL, Burnham S, Bourgeat P, et al. Amyloid β deposition, neurodegeneration, and cognitive decline in sporadic Alzheimer's disease: a prospective cohort study. *Lancet Neurol.* 2013;12:357-367. doi:10.1016/S1474-4422(13)70044-9
- van Dyck CH, Swanson CJ, Aisen P, et al. Lecanemab in Early Alzheimer's Disease. *N Engl J Med.* 2023;388:9-21. doi:10.1056/NEJMoa2212948
- Mintun MA, Lo AC, Duggan Evans C, et al. Donanemab in Early Alzheimer's Disease. *N Engl J Med.* 2021;384:1691-1704. doi:10.1056/NEJMoa2100708
- Sims JR, Zimmer JA, Evans CD, et al. Donanemab in Early Symptomatic Alzheimer Disease: the TRAILBLAZER-ALZ 2 randomized clinical trial. *JAMA.* 2023;330(6):512-527. doi:10.1001/jama.2023.13239
- Rafii MS, Sperling RA, Donohue MC, et al. The AHEAD 3-45 Study: design of a prevention trial for Alzheimer's disease. *Alzheimers Dement.* 2023;19(4):1227-1233. doi:10.1002/alz.12748
- Sperling RA, Donohue MC, Raman R, et al. Trial of solanezumab in preclinical Alzheimer's disease. *N Engl J Med.* 2023;389:1096-1107. doi:10.1056/NEJMoa2305032
- Huang L-K, Chao S-P, Hu C-J. Clinical trials of new drugs for Alzheimer disease. *J Biomed Sci.* 2020;27:18. doi:10.1186/s12929-019-0609-7
- McMillan CT, Chételat G. Amyloid "accumulators": the next generation of candidates for amyloid-targeted clinical trials? *Neurology.* 2018;90:759-760. doi:10.1212/WNL.00000000000005362
- Pemberton HG, Collij LE, Heeman F, et al. Quantification of amyloid PET for future clinical use: a state-of-the-art review. *Eur J Nucl Med Mol Imaging.* 2022; 49:3508-3528. doi:10.1007/s00259-022-05784-y
- Farrell ME, Chen X, Rundle MM, Chan MY, Wig GS, Park DC. Regional amyloid accumulation and cognitive decline in initially amyloid-negative adults. *Neurology.* 2018;91:e1809-e1821. doi:10.1212/WNL.0000000000006469
- Landau SM, Horng A, Jagust WJ. Initiative F the ADN. Memory decline accompanies subthreshold amyloid accumulation. *Neurology.* 2018;90:e1452-e1460. doi:10.1212/WNL.00000000000005354
- Collij LE, Mastenbroek SE, Salvadó G, et al. Regional amyloid accumulation predicts memory decline in initially cognitively unimpaired individuals. *Alzheimers Dement Diagn Assess Dis Monit.* 2021;13:e12216. doi:10.1002/dad2.12216
- Langford O, Raman R, Sperling RA, Cummings J, Sun C-K, Jimenez-Maggiara G, et al. Predicting amyloid burden to accelerate recruitment of secondary prevention clinical trials. *J Prev Alzheimers Dis.* 2020;7:213-218. doi:10.14283/jpad.2020.44
- Budd Haeberlein S, Aisen PS, Barkhof F, et al. Two randomized phase 3 studies of aducanumab in early Alzheimer's disease. *J Prev Alzheimers Dis.* 2022;9:197-210. doi:10.14283/jpad.2022.30
- Shcherbinin S, Evans CD, Lu M, et al. Association of amyloid reduction after donanemab treatment with tau pathology and clinical outcomes: the TRAILBLAZER-ALZ randomized clinical trial. *JAMA Neurol.* 2022;79:1015-1024. doi:10.1001/jamaneurol.2022.2793
- Klunk WE, Koeppe RA, Price JC, et al. The Centiloid project: standardizing quantitative amyloid plaque estimation by PET. *Alzheimers Dement J Alzheimers Assoc.* 2015;11:1-15.e4. doi:10.1016/j.jalz.2014.07.003
- Landau SM, Fero A, Baker SL, et al. Measurement of longitudinal β -amyloid change with 18F-florbetapir PET and standardized uptake value ratios. *J Nucl Med.* 2015;56:567-574. doi:10.2967/jnumed.114.148981
- Rowe C, Doré V, Thurfjell L, et al. Longitudinal assessment of A β accumulation in non-demented individuals: a 18F-flutemetamol study. *J Nucl Med.* 2015;56:193.
- Bourgeat P, Doré V, Doecke J, et al. Non-negative matrix factorisation improves Centiloid robustness in longitudinal studies. *Neuroimage.* 2021;226:117593. doi:10.1016/j.neuroimage.2020.117593
- Bourgeat P, Doré V, Burnham SC, et al. β -amyloid PET harmonisation across longitudinal studies: application to AIBL, ADNI and OASIS3. *Neuroimage.* 2022;262:119527. doi:10.1016/j.neuroimage.2022.119527
- Lowe SL, Duggan Evans C, Shcherbinin S, et al. Donanemab (LY3002813) Phase 1b Study in Alzheimer's disease: rapid and sustained reduction of brain amyloid measured by Florbetapir F18 imaging. *J Prev Alzheimers Dis.* 2021;8:414-424. doi:10.14283/jpad.2021.56
- Klein G, Delmar P, Voyle N, et al. Gantenerumab reduces amyloid- β plaques in patients with prodromal to moderate Alzheimer's disease: a PET substudy interim analysis. *Alzheimers Res Ther.* 2019;11:101. doi:10.1186/s13195-019-0559-z
- Luckett ES, Schaefferbeke J, De Meyer S, et al. Longitudinal changes in 18F-Flutemetamol amyloid load in cognitively intact APOE4 carriers versus noncarriers: methodological considerations. *NeuroImage Clin.* 2023;37:103321. doi:10.1016/j.nicl.2023.103321
- Jack CR, Wiste HJ, Weigand SD, et al. Defining imaging biomarker cut points for brain aging and Alzheimer's disease. *Alzheimers Dement.* 2017;13:205-216. doi:10.1016/j.jalz.2016.08.005
- Farrell M. Defining the lowest threshold for amyloid-PET to predict future cognitive decline and amyloid accumulation | neurology. *Neurology.* 2021;96(4):e619-e631. doi:10.1212/WNL.00000000000011214
- Smith AM, Obuchowski NA, Foster NL, et al. The RSNA QIBA profile for amyloid PET as an imaging biomarker for cerebral amyloid quantification. *J Nucl Med.* 2023;64:294-303. doi:10.2967/jnumed.122.264031
- Life Radiopharma Berlin GmbH. *Neuraceq: EPAR—Product Information.* EMEA/H/C/002553. Eur Med Agency; 2022. <https://www.ema.europa.eu/en/medicines/human/EPAR/neuraceq>
- GE Healthcare. *Vizamyl: EPAR—Product Information.* EMEA/H/C/002557. Eur Med Agency; 2023. <https://www.ema.europa.eu/en/medicines/human/EPAR/vizamyl>
- Eli Lilly. *Amyvid: EPAR—Product Information.* EMEA/H/C/002422. Eur Med Agency; 2021. <https://www.ema.europa.eu/en/medicines/human/EPAR/amyvid>
- Amadoru S, Doré V, McLean CA, et al. Comparison of amyloid PET measured in Centiloid units with neuropathological findings in Alzheimer's disease. *Alzheimers Res Ther.* 2020;12:22. doi:10.1186/s13195-020-00587-5
- La Joie R, Ayakta N, Seeley WW, et al. Multisite study of the relationships between *antemortem* [11 C]PIB-PET Centiloid values and *post-mortem* measures of Alzheimer's disease neuropathology. *Alzheimers Dement.* 2019;15:205-216. doi:10.1016/j.jalz.2018.09.001
- Reinartz M, Luckett ES, Schaefferbeke J, et al. Classification of 18F-Flutemetamol scans in cognitively normal older adults using machine learning trained with neuropathology as ground truth. *Eur J Nucl Med Mol Imaging.* 2022;49:3772-3786. doi:10.1007/s00259-022-05808-7
- Collij LE, Salvadó G, Shekari M, et al. Visual assessment of [18F]flutemetamol PET images can detect early amyloid pathology and grade its extent. *Eur J Nucl Med Mol Imaging.* 2021;48:2169-2182. doi:10.1007/s00259-020-05174-2
- Cho SH, Choe YS, Kim HJ, et al. A new Centiloid method for 18F-florbetaben and 18F-flutemetamol PET without conversion to PIB. *Eur J Nucl Med Mol Imaging.* 2020;47:1938-1948. doi:10.1007/s00259-019-04596-x
- Su Y, Hornbeck RC, Speidel B, et al. Comparison of Pittsburgh compound B and florbetapir in cross-sectional and longitudinal studies. *Alzheimers Dement Diagn Assess Dis Monit.* 2019;11:180-190. doi:10.1016/j.dadm.2018.12.008
- Su Y, Flores S, Hornbeck RC, et al. Utilizing the Centiloid scale in cross-sectional and longitudinal PIB PET studies. *NeuroImage Clin.* 2018;19:406-416. doi:10.1016/j.nicl.2018.04.022

37. Matsuda H, Ito K, Ishii K, et al. Quantitative evaluation of 18F-flutemetamol PET in patients with cognitive impairment and suspected Alzheimer's disease: a multicenter study. *Front Neurol*. 2021;11:578753.
38. Salvadó G, Molinuevo JL, Brugulat-Serrat A, et al. Centiloid cut-off values for optimal agreement between PET and CSF core AD biomarkers. *Alzheimers Res Ther*. 2019;11:27. doi:10.1186/s13195-019-0478-z
39. Tudorascu DL, Minhas DS, Lao PJ, et al. The use of Centiloids for applying [¹¹C]PiB classification cutoffs across region-of-interest delineation methods. *Alzheimers Dement Diagn Assess Dis Monit*. 2018;10:332-339. doi:10.1016/j.dadm.2018.03.006
40. Lopes Alves I, Collij LE, Altomare D, et al. Quantitative amyloid PET in Alzheimer's disease: the AMYPAD prognostic and natural history study. *Alzheimers Dement*. 2020;16:750-758. doi:10.1002/alz.12069
41. Collij LE, Farrar G, Valléz García D, et al. The amyloid imaging for the prevention of Alzheimer's disease consortium: a European collaboration with global impact. *Front Neurol*. 2023;13:1063598.
42. Lane CA, Parker TD, Cash DM, et al. Study protocol: insight 46 – a neuroscience sub-study of the MRC National Survey of Health and Development. *BMC Neurol*. 2017;17:75. doi:10.1186/s12883-017-0846-x
43. Shekari M, Verwer EE, Yaqub M, et al. Harmonization of brain PET images in multi-center PET studies using Hoffman Phantom Scan. 2023;10:68. doi:10.1186/s40658-023-00588-x
44. Burgos N, Cardoso MJ, Thielemans K, et al. Attenuation correction synthesis for hybrid PET-MR scanners: application to brain studies. *IEEE Trans Med Imaging*. 2014;33:2332-2341. doi:10.1109/TMI.2014.2340135
45. Grecchi E, Foley C, Gispert JD, Wolz R. P3-434: Centiloid Pet Suvr analysis using the supratentorial white matter as reference region. *Alzheimers Dement*. 2018;14:P1278. doi:10.1016/j.jalz.2018.06.1797
46. Coath W, Modat M, Cardoso MJ, et al. Operationalising the Centiloid Scale for [¹⁸F]florbetapir PET Studies on PET/MR. *Radiology and Imaging*; 2022. doi:10.1101/2022.02.11.22270590
47. Keshavan A, Wellington H, Chen Z, et al. Concordance of CSF measures of Alzheimer's pathology with amyloid PET status in a preclinical cohort: a comparison of Lumipulse and established immunoassays. *Alzheimers Dement Diagn Assess Dis Monit*. 2021;13(1):e12131. doi:10.1002/dad2.12131
48. Lu K, Nicholas JM, Collins JD, et al. Cognition at age 70: life course predictors and associations with brain pathologies. *Neurology*. 2019;93:e2144-e2156. doi:10.1212/WNL.0000000000008534
49. Saito T, Rehmsmeier M. The precision-recall plot is more informative than the ROC plot when evaluating binary classifiers on imbalanced datasets. *PLoS One*. 2015;10:e0118432. doi:10.1371/journal.pone.0118432
50. Villain N, Chételat G, Grassiot B, et al. Regional dynamics of amyloid- β deposition in healthy elderly, mild cognitive impairment and Alzheimer's disease: a voxelwise PiB – PET longitudinal study. *Brain*. 2012;135:2126-2139. doi:10.1093/brain/aws125
51. Zammit MD, Tudorascu DL, Laymon CM, et al. PET measurement of longitudinal amyloid load identifies the earliest stages of amyloid-beta accumulation during Alzheimer's disease progression in Down syndrome. *Neuroimage*. 2021;228:117728. doi:10.1016/j.neuroimage.2021.117728
52. Chen K, Roontiva A, Thiyyagura P, et al. Improved power for characterizing longitudinal amyloid- β PET changes and evaluating amyloid-modifying treatments with a cerebral white matter reference region. *J Nucl Med*. 2015;56:560-566. doi:10.2967/jnumed.114.149732
53. Brendel M, Högenauer M, Delker A, et al. Improved longitudinal [18F]-AV45 amyloid PET by white matter reference and VOI-based partial volume effect correction. *Neuroimage*. 2015;108:450-459. doi:10.1016/j.neuroimage.2014.11.055
54. Hanseeuw BJ, Malotau V, Dricot L, et al. Defining a Centiloid scale threshold predicting long-term progression to dementia in patients attending the memory clinic: an [18F] flutemetamol amyloid PET study. *Eur J Nucl Med Mol Imaging*. 2021;48:302-310. doi:10.1007/s00259-020-04942-4
55. Lopes Alves I, Heeman F, Collij LE, et al. Strategies to reduce sample sizes in Alzheimer's disease primary and secondary prevention trials using longitudinal amyloid PET imaging. *Alzheimers Res Ther*. 2021;13:82. doi:10.1186/s13195-021-00819-2
56. Burnham SC, Laws SM, Budgeon CA, et al. Impact of APOE- ϵ 4 carriage on the onset and rates of neocortical A β -amyloid deposition. *Neurobiol Aging*. 2020;95:46-55. doi:10.1016/j.neurobiolaging.2020.06.001
57. Mishra S, Blazey TM, Holtzman DM, et al. Longitudinal brain imaging in preclinical Alzheimer disease: impact of APOE ϵ 4 genotype. *Brain*. 2018;141:1828-1839. doi:10.1093/brain/awy103
58. Betthausen TJ, Kosciak RL, Jedynak BM, et al. Multi-method investigation of factors influencing amyloid onset and impairment in three cohorts. *Brain*. 2022;145(11):4065-4079.
59. Nelson ME, Jester DJ, Petkus AJ, Andel R. Cognitive reserve, alzheimer's neuropathology, and risk of dementia: a systematic review and meta-analysis. *Neuropsychol Rev*. 2021;31:233-250. doi:10.1007/s11065-021-09478-4
60. Lee DH, Seo SW, Roh JH, et al. Effects of cognitive reserve in Alzheimer's disease and cognitively unimpaired individuals. *Front Aging Neurosci*. 2022;13:784054. doi:10.3389/fnagi.2021.784054

SUPPORTING INFORMATION

Additional supporting information can be found online in the Supporting Information section at the end of this article.

How to cite this article: Bollack A, Collij LE, García DV, et al. Investigating reliable amyloid accumulation in Centiloids: Results from the AMYPAD Prognostic and Natural History Study. *Alzheimer's Dement*. 2024;1-13. <https://doi.org/10.1002/alz.13761>